Nanomaterials and Nanotechnology

OPEN ACCESS
ARTICLE

Preparation of CdO Rhombus-like Nanostructure and Its Photocatalytic Degradation of Azo Dyes from Aqueous Solution

Regular Paper

Azadeh Tadjarodi[1,*], Mina Imani[1], Hamed Kerdari[2], Keyvan Bijanzad[1], Dorsan Khaledi[1] and Maryam Rad[1]

1 Research Laboratory of Inorganic Materials Synthesis, Department of Chemistry, Iran University of Science and Technology, Tehran, Iran
2 Department of Chemistry, Saveh Branch, Islamic Azad University, Saveh, Iran
* Corresponding author E-mail: tajarodi@iust.ac.ir

Received 4 Dec 2013; Accepted 11 Mar 2014

DOI: 10.5772/58464

Abstract In this work, a special rhombus-like structure of CdO composed of particles at the nanometre scale was successfully synthesized for the first time. A facile hydrothermal process with a post-reaction calcination was employed to prepare this nanomaterial. Scanning electron microscopy (SEM) images showed that the obtained rhombus-like structure consists of nanoparticles with an average size of 29 nm. The band gap energy of 1.9 eV based on a diffuse reflectance spectroscopy (DRS) showed that the product can be favourable to photoactivity in the visible region of sunlight. The prepared sample was employed to destruct carcinogenic azo dyes, such as Congo Red (CR), Malachite Green (MG) and Crystal Violet (CV). The obtained results showed that the CdO with the special morphology was able to effectively catalyse the degradation of these pollutants. The related decolourization efficiencies were obtained by up to 100% after various lengths of time of light irradiation. It was concluded that the photodegradation of the mentioned organic dyes under visible light irradiation by a CdO rhombus-like nanostructure follows the first-order reaction kinetics. The effect of the initial pH and contact time on the percentage of the decolourization of these organic dyes was also studied.

Keywords Photodegradation, Nanostructures, Oxides

1. Introduction

A major challenge we deal with in industries such as textiles, food, paper, cosmetics and so on has always been refining toxic contaminants before discharging them into the environment [1, 2]. The techniques used to eliminate coloured contaminants from wastewaters are as follows: coagulation, flocculation, membrane filtration and adsorption [3-6]. One of the most effective and applicable methods for the elimination or abatement of

environmental pollutants is a photocatalysis procedure. This method has developed thanks to the growth of nano-science and nanotechnology. Nano-sized semiconductor photocatalysts have attracted a lot of attention because of their optical and electrical properties, and so many investigations have focused on this field [7-9]. Cadmium oxide (CdO) is a known n-type semiconductor with a direct and indirect band gap energy of 2.2-2.5 eV and 1.36-1.98 eV, respectively [10-13]. In fact, the lattice's defects in the crystalline structure lead to a diversity in the band gap energy [14]. This material has been synthesized using numerous methods as follows: microemulsion [11], chemical vapour deposition [14], sol-gel process [15, 16], sonochemical technique [17], hydrothermal/solvothermal method [18-20] and mechanochemical process [21, 22]. This compound not only has unique optical and optoelectrical characteristics but it also has selective catalytic properties that make the compound suitable for use in the photodegradation of toxic organic compounds, dyes, pigments and other environmental pollutants [23-28]. Azo dyes are toxic contaminants and even carcinogenic for living organisms. Therefore, it is essential that these pollutants be removed before being discharged into the environment. Despite the fact that Congo Red, Malachite Green and Crystal Violet dyes are hazardous azo dyes, they are still used in various industries. Thus, it is vital to convert them into non-toxic species. Scheme 1 indicates the molecular structures of these dyes [29, 30]. Many studies have reported the use of one specific semiconductor for the photodegradation of cationic and anionic azo dyes, separately [31-34]. These reports prompted us to evaluate the photocatalytic performance of the synthesized semiconductor for the degradation of both cationic and anionic azo dyes. Our study of the photocatalytic activity of a single semiconductor on the decontamination of the both cationic and anionic dyes was the first of its kind [35]. In this study, we focused on the synthesis, photocatalytic activity and reuse capability of another special morphology of this metal oxide. As a matter of fact, a case study examining the special CdO nanostructure's ability to photodegrade coloured pollutants has not been reported, yet. The toxic organic dyes (Congo Red, Malachite Green, and Crystal Violet) were selected as models of wastewater pollutants. The resulting product was characterized by using FT-IR, XRD, TGA and SEM techniques.

2. Experimental section

2.1 Materials of the synthesis

Cadmium chloride monohydrate ($CdCl_2$. H_2O, Merck, pure), ammonium oxalate monohydrate ($(NH_4)_2.C_2O_4.H_2O$, Merck, 99% purity), sodium hydroxide (NaOH, Merck, 99.99% purity) were supplied as initial reagents to synthesize the CdO nanostructure. Congo Red (sodium 3,3'-([1,1'-biphenyl]-4,4'-diyl)bis(4-aminonaphthalene-1-sulfonate) Malachite Green (4-[(4-dimethylaminophenyl)phenyl-methyl]-N,N-dimethylaniline) and Crystal Violet (Tris (4-(dimethylamino)phenyl) methylium chloride) were used as model dyes. Deionized and distilled water were used to prepare all the solutions.

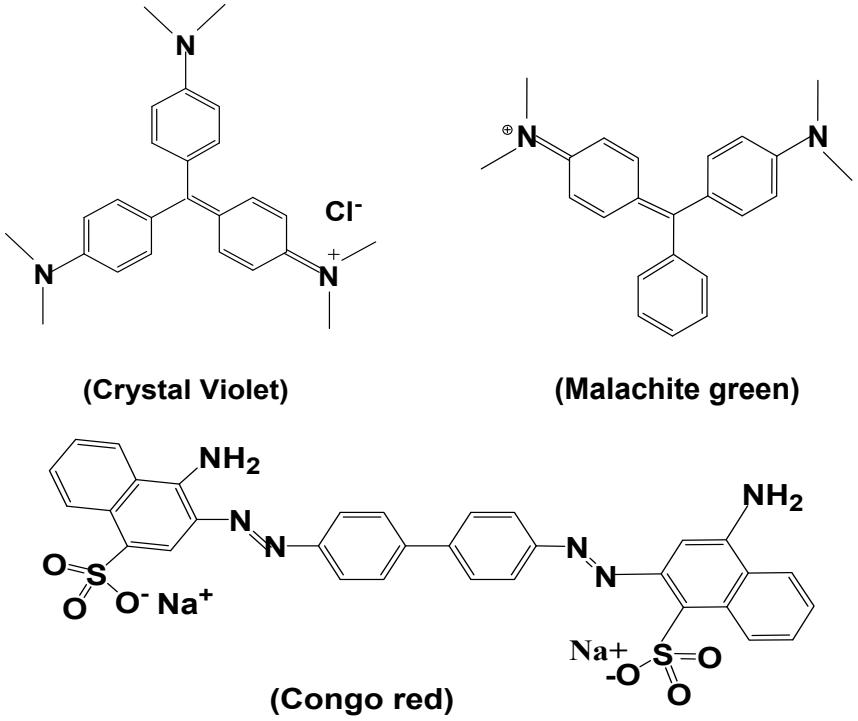

Scheme 1. Molecular structures of Congo Red (CR), Crystal Violet (CV), Malachite Green (MG) dyes

2.2 Characterization

Powder X-ray diffraction (XRD) measurements were carried out using a JEOL diffractometer with monochromatized Cu Kα radiation (λ =1.5418 Å). Fourier transform infrared (FT-IR) spectra were recorded on a Shimadzu-8400S spectrometer in the range of 400-4000 cm^{-1} using KBr pellets. Scanning electron microscopy (SEM) images were obtained on a Philips (XL-30) with gold coating. Thermogravimetric analysis (TGA) measurements were carried out on a NETZSCH TG 209 F1 Iris apparatus with a heating rate of 10 °C min^{-1} under a nitrogen atmosphere. The optical absorption and transmission of the CdO nanostructure were evaluated in the range of 190-800 nm by using a UV–Vis spectrophotometer (Shimadzu-UV-2550-8030, light source with a wavelength of 360.0 nm) at room temperature. A double-beam UV spectrophotometer (Shimadzu UV-1700) was used for the determination of CR, MG and CV concentrations in the supernatant solutions before and after the photocatalytic reaction.

2.3 Synthesis method

In order to synthesize the CdO rhombus-like structure, $CdCl_2$. H_2O (0.40 g) and $(NH_4)_2.C_2O_4.H_2O$ (0. 28 g) were dissolved in 30 mL of distilled water at an alkaline pH as starting materials with a molar ratio of 1:1. Alkaline conditions were obtained by adding 1.5 M of NaOH solution under ultrasonic waves for 30 min so that the pH reached 11. The resulting solution was transferred into an 80 mL Teflon-lined stainless steel autoclave to carry out the hydrothermal reaction at 160 °C for 24 h. The autoclave was cooled down to room temperature. The resulting precursor was filtered, washed with distilled water and ethanol several times to remove additional ions, and finally dried at 70 °C for 24 h in open air overnight. Then, the resulting precipitation (precursor) was calcined at 450 °C for 2 h in a furnace to obtain the final product (CdO).

2.4 Photocatalytic activity

The photocatalytic activity of the CdO specimen was measured by degrading a series of azo dyes, such as CR, MG and CV in aqueous solution under visible light irradiation. In order to establish the adsorption-desorption equilibrium, each beaker containing CdO powder and related dye solution was left in the dark and magnetically stirred for 45 min before the photocatalytic reaction began. In the photocatalytic experiments, a certain amount (0.01 g) of photocatalyst was separately poured into a 50 mL beaker containing 25 mL of related dye solution with an initial concentration of 5 mg L^{-1}. The suspension was magnetically stirred for 4 h under visible light irradiation. The effect of the pH on the elimination of the dyes was evaluated by adjusting the pH of the solution to 5, 6, 8 and 9 using 0.01 mol L^{-1} HCl or NaOH. The visible irradiation was supplied by a high-pressure mercury-vapour lamp (500W and λ=546.8 nm). At given intervals of irradiation (1 h), portions of the suspension were removed from the reaction vessel and separated using centrifuge then analysed by UV-Vis spectrophotometer. Next, the remaining concentration of CR, MG and CV solutions was studied using a UV-Vis spectrophotometer at wavelengths of 498, 617 and 590 nm, respectively.

3. Results and Discussion

3.1 Structural study

Figure 1 shows the FT-IR spectra of the obtained precursor from the hydrothermal reaction (Figure 1a) and the resulting product of the calcination at 450 °C for 2 h (Figure 1b). The observed peaks in Figure 1a are related to the organic groups of the precursor. Probably, the absorption bands at 3454 and 3321 cm^{-1} can be attributed to the N-H antisymmetrical and symmetrical stretching vibrations of the residual by-product, respectively. The overlapping of the O-H vibration band of the H_2O molecule with these frequencies can lead to a broadening of these bands. The peaks that appeared at 1606 and 1307 cm^{-1} are assigned to C=O and C-O stretching vibrations of the carbonyl groups, respectively. Actually, the frequency of the CO vibrations was decreased by the resonance effect. The peaks observed at 904, 759 and 491 cm^{-1} can be attributed to the ν(CO) and $\nu(CO_2)$ [36-38]. Likewise, the peak that appeared at 673 cm^{-1} can be ascribed to the vibration band of the Cd-O bond formed in the precursor [39]. As a result of the heat treatment at 450 °C, the typical peaks of the organic molecules of the precursor disappeared (Figure 1b). Obviously, the organic section was removed and only a broad band remained representing the CdO formation.

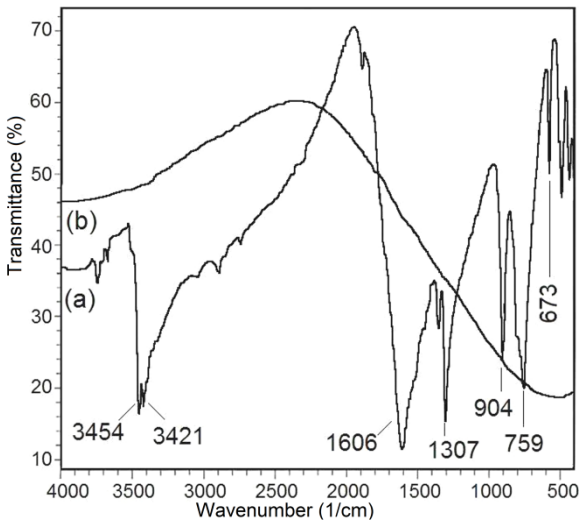

Figure 1. FT-IR spectra of the precursor: (a) as the intermediate molecule prepared by hydrothermal reaction and (b) the resultant CdO after calcinating treatment at 450 °C for 2 h.

$$CdCl_2.H_2O + (NH_4)_2C_2O_4.H_2O \xrightarrow[2NaOH,\ pH=11]{\text{Hydrothermal reaction [160 °C , 24 h]}}$$

$$[Cd(C_2O_4).(H_2O)]_{(s)} + 2NH_4OH_{(aq)} + 2NaCl_{(aq)} + H_2O_{(aq)} \xrightarrow[450\ °C\ ,\ 2\ h]{\text{Filtration, Calcination}}$$

(precursor)

$$\mathbf{CdO}_{(s)} + H_2O_{(g)} + CO_{2\ (g)} + CO_{(g)}$$

(product)

Scheme 2. Schematic of the proposed mechanism for CdO formation under hydrothermal conditions

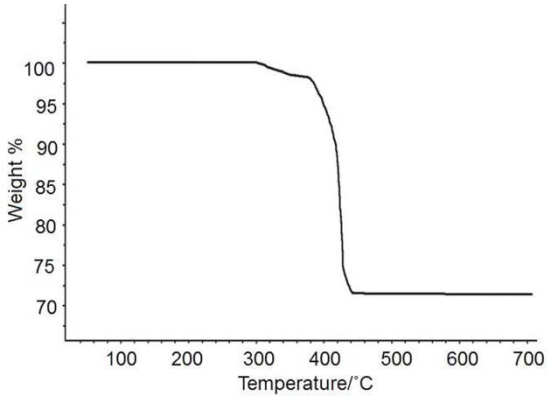

Figure 2. The curve of the thermal gravimetric analysis (TGA) of the precursor

According to the FT-IR data, we can propose probable reactions for the formation of the intermediate molecule (precursor) and CdO as the product resulting from the hydrothermal reaction, which is shown in Scheme 2.

Figure 2 illustrates the curve of the thermal gravimetric analysis of the precursor. According to this curve, the decay of this compound is performed in a two-step pattern of weight loss. The first weight loss of 1.8% is observed in the temperature range of between 300 – 380 °C, which can be related to the decomposition of adsorbed water molecules. The second weight loss of 29.66% observed in the temperature range between 380-450°C can be attributed to the decomposition of the organic sections in the precursor. It was found that the weight loss terminates at 450 °C, so this temperature was determined as the calcination temperature of the precursor molecules and reached the CdO phase.

Figure 3 shows X-ray diffraction patterns of the resulting products before and after calcination treatment. The XRD pattern of the intermediate molecule (Figure 3a) demonstrates the formation of cadmium oxalate monohydrate compound in a close agreement to the reference pattern of No. 022-1064. After the calcination process, the obtained Cd-containing precursor is altered to the CdO phase (Figure 3b). This pattern confirms the formation of the CdO phase with a lattice parameter a=4.695 Å. The diffraction peaks at 2θ values of 33.01°, 38.20°, 55.20°, 65.80°, and 69.20° associated with the 111, 200, 220, 311, and 222 planes of the cubic phase of the CdO (JCPDS- 05-0640). No other peaks related to the impurities were detected.

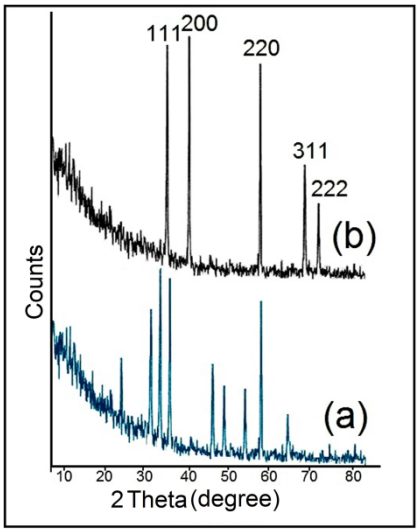

Figure 3. XRD patterns of the obtained intermediate molecule (a) and CdO phase (b)

3.2 Morphological study

Figure 4 reveals the SEM images of the CdO nanostructure obtained. The low magnification images of SEM (Figures 4a and 4b) clearly indicate rhombus-like structures with regular facets and sharp edges between the facets. Meanwhile, a high magnification of SEM images shown in Figure. 4c, 4d and 4e revealed that the structure mentioned consists of the particles at the nanoscale with an average size of 29 nm. It is found that the special orientation of the nanoparticles can be aggregated into a rhombus form. Probably, the coordination mode of the ligand molecules (oxalate ions) to metal ions (cadmium ions) in the precursor can lead to this orientation before the calcining treatment, which confirms the FT-IR and XRD data, and the proposed mechanism.

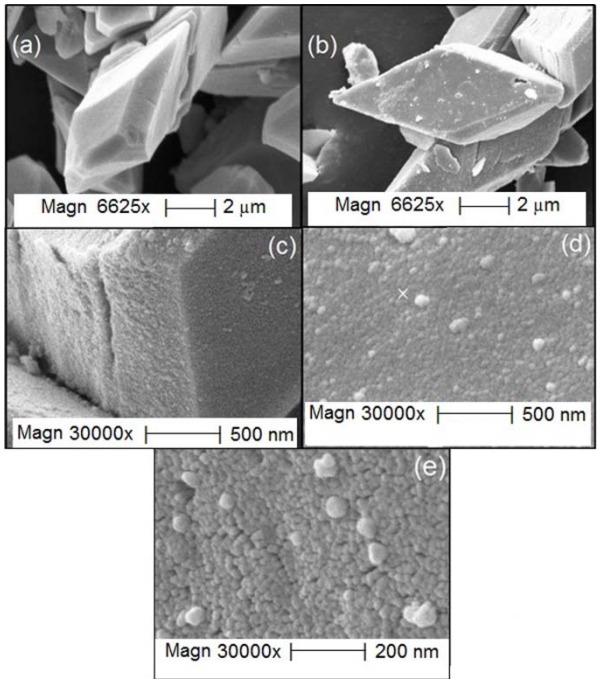

Figure 4. SEM images of the CdO rhombus nanostructure obtained from the hydrothermal reaction

3.3 Photocatalytic activity of the CdO rhombus nanostructure

The photoactivity of the prepared CdO nanostructure was studied by degrading CR, MG and CV, the carcinogenic organic dyes, in an aqueous medium under visible light irradiation. The band gap energy estimation of the prepared nano-sized oxide, 1.9 eV, showed that the photodegradation behaviour of the product is activated in the visible light domain. The optical absorption edge (Eg) is determined by the following equation:

$$(\alpha h\nu)^2 = B(h\nu - E_g) \qquad \text{(Eq. (1))}$$

where, hν is the photon energy, α is the absorption coefficient, B is a constant value and E_g represents the band gap energy [40]. By plotting the $(\alpha h\nu)^2$ *vs*. hν in eV and obtaining the extrapolation point of this curve, the band gap energy of the product can be determined. Figure 5 shows the band gap energy plot of CdO based on the diffuse reflectance spectrum (DRS) of solid state UV-Vis (in the inset of this Figure).

A wide range of band gap energy values was found for the semiconducting materials. This diversity in the values of the optical absorption edge can be attributed to the defects induced by the synthesis conditions, structural morphology and the particle size of the product [41-42].

The band gap energy of cadmium oxide was reported as being in the range of 2.2-2.5 eV. The different band gaps were presented for the various morphologies of CdO. In fact, one way of varying the band gap energy is by synthesizing new structures with special morphologies so that the absorption edge can shift to small or large values. Therefore, the band gap value can be tuned to an extended range from 1.1 eV to 3.4 eV [10, 43-44].

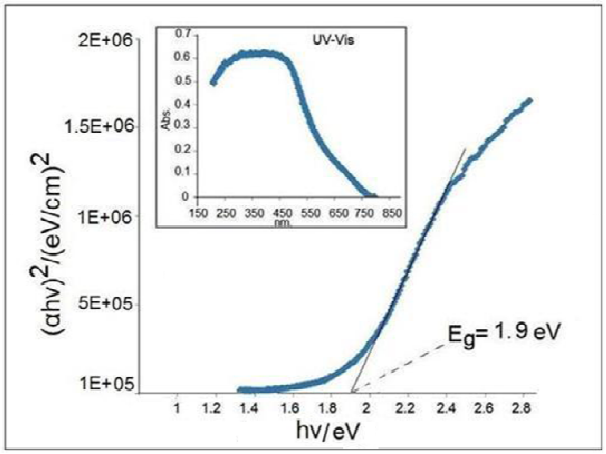

Figure 5. Optical absorption edge of the CdO rhombus structure with DRS spectrum in the inset

The synthesis of the special rhombus-like microstructure led to a red shift of the optical absorption edge of the CdO, which may mark this product out for interesting applications.

3.3.1 Initial pH effect

The initial pH effect for depredating the mentioned organic azo dyes in water was investigated by adjusting the pH to various amounts, namely of 5, 6, 8 and 9 by using 0.01 mol.L^{-1} HCl or NaOH. Figure 6 shows that the degradation percentages of these coloured pollutants reach the highest value when the solution pH is adjusted to 6 for each run. This pH is very close to natural pH so all of the experiments were performed in a solution with a neutral pH. It is concluded that the presence of excess charges at the low and high pH values, and the production of an electrostatic repulsion lead to the adsorbing sites being occupied by the produced cationic and anionic species, and to a reduction in the adsorption of organic molecules on the active sites of the sample. Subsequently, this decreases the degradation efficiency of pollutants on the surface of the photocatalyst.

3.3.2 Contact time

Decolourization efficiencies were calculated based on the absorption spectra intensity of the CR, MG and CV solutions at different times. In addition, the decolourizing efficiency was inferred from Eq. (2):

$$\text{efficiency} = \frac{C0 - Ci}{C0} \times 100\% \qquad \text{(Eq. (2))}$$

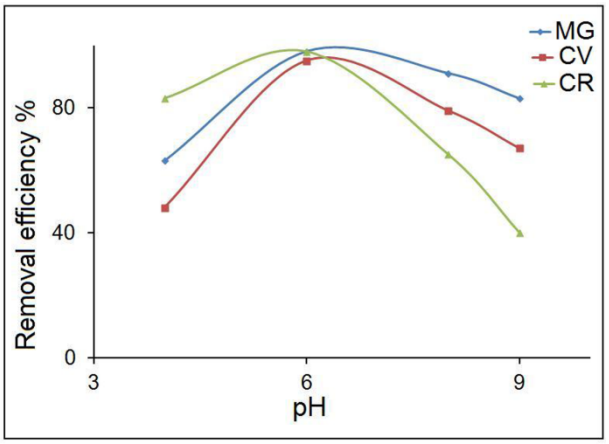

Figure 6. The amount of azo dyes removed at various pHs

where, C_0 is the initial concentration of the dye before the reaction, and C_i is the concentration of the dye after the treatment with CdO rhombus particles at various illumination times (0-4 h). No degradation of azo dyes was observed in the absence of a photocatalyst under visible light irradiation. The MG and CV concentrations did not decrease once adsorption-desorption had reached an equilibrium; however, the CR concentration decreased by about 5%. When the photocatalytic activity of the prepared CdO was evaluated, this partial adsorption on photocatalyst sites was eliminated. According to Figure 7, at the first hour of light irradiation, decolourizing efficiencies for MG and CR dye solutions with concentration of 5 mg. L^{-1} were achieved of about 98 and 94%, respectively. These values nearly reached 100% after 2h illumination. This result proves that the synthesized photocatalyst performs excellently in removing the mentioned azo dyes under visible light illumination in a short time. Moreover, in the same interval of illumination time (1h), another dye solution (CV) was destructed by CdO rhombus particles by about 15%. The photocatalytic process was prolonged for a few more hours and the maximum degradation of CV dye reached 95% after 4h. To estimate the ability of this type of photocatalyst, a CR solution with a higher concentration (50 mg. L^{-1}) was treated with a small amount of CdO rhombus particles. It was found that the CdO as-prepared, was able to effectively catalyse the degradation of the concentrated solution of CR dye after 4h of light irradiation. The adsorption of dye molecules on the active sites of the catalyst surface with the individual structures plays an important role in facilitating the transportation of the charge and the efficiency of the removal. The construction of such a structure with a rhombus-like architecture can improve the adsorption of dye species leading to an increase in the removal efficiency [45, 46].

In order to evaluate the reusability of this semiconductor, a series of experiments were designed and catalyst particles were reused three times under similar conditions. Before each experiment, the catalyst was collected, centrifuged, washed with acetone and deionized water to remove the adsorbed species, dried, and performed again. Figure 8 indicates the reusability of the CdO nanostructure for the photodegradation of the selected pollutants during the three treatment times. The results presented not much more decrease in the decolourizing efficiency, which demonstrates the stable behaviour of this product for further photodegradation cycles on the water treatment.

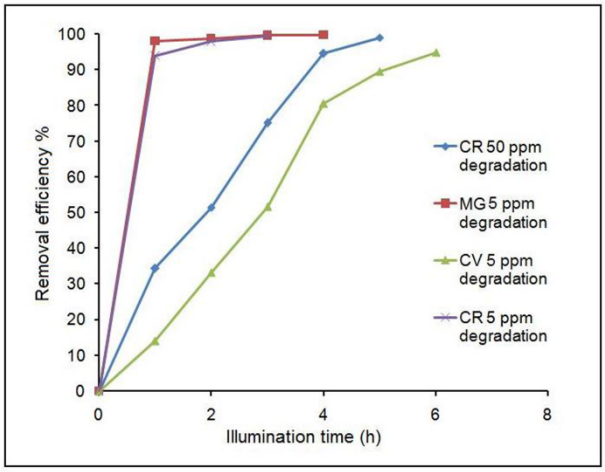

Figure 7. Decolourizing efficiencies for MG, CV and CR dye solutions with concentration of 5 mg. L^{-1} and illumination times (0-6 h)

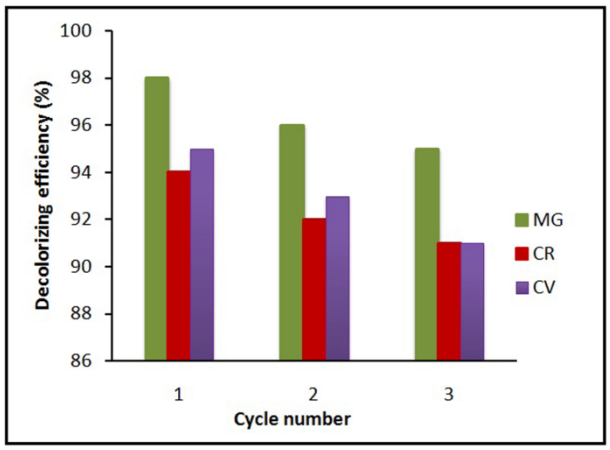

Figure 8. Reusability of CdO rhombus nanostructure for the photodegradation of the selected azo dyes

3.3.3 The reaction kinetics

The time difference in the decolourization efficiencies of the mentioned dyes can be ascribed to the reaction kinetics of each colour. Figure 9 indicates that there is a linear relationship between $Ln(C_0/C_t)$ versus reaction time, t. This result reveals that the photocatalytic degradation of azo dyes in an aqueous CdO suspension can be described by the first-order kinetic model as follows:

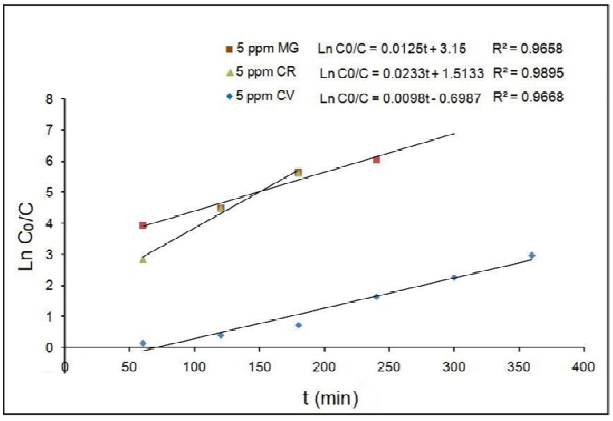

Figure 9. Photocatalytic activity of the prepared photocatalyst (CdO rhombus nanostructure) degrading Congo Red, Crystal Violet and Malachite Green under visible irradiation

$$Ln\ (\frac{C\,0}{C\,t}) = kt \qquad \text{(Eq.(3))}$$

where C_0 is the initial concentration (mM) and C_t is the instantaneous concentration of the mentioned dyes, the slope, k, is the apparent rate constant. According to the diagram, the rate constants of photodegradation reactions for CR, MG and CV dyes are 0.0233, 0.0125 and 0.0098 min^{-1}, respectively. These findings demonstrated that the photodegradation of the CR dye occurred before the CV and MG dyes. CV dye, among these three chemical pigments, was removed from the aqueous solution later than the others during the photocatalytic process. This delay may be due to CV dye's complicated structure in comparison with CR and MG dyes.

3.3.4 Photodegradation mechanism

Scheme 3 represents the photocatalytic mechanism of the prepared product. At first, the photocatalytic behaviour of the prepared CdO nanostructure was studied in order to develop a mechanism to decolourize cationic azo dyes, such as Malachite Green and Crystal Violet under visible light irradiation. Then, the capability of this semiconductor to remove Congo Red as an anionic dye was examined. With regard to semiconductor photocatalysts, physical and chemical mechanisms have previously been reported in the literature. Although the Crystal Violet and Malachite Green are cationic dyes and Congo Red is an anionic dye, the photodegradation actually originated from the hydroxyl (•OH) and superoxide anions ($O_2^{\bullet-}$) radicals resulting from the formation of (e^-/h^+) pairs in semiconductors [47]. As the catalyst surface is photo-excited, the production of electrons in conduction bands (e^-) and holes in valance bands (h^+) lead to transfers of charges on the photocatalyst sites. Its particular morphology increases the adsorption process of dye molecules on the surface of the catalyst. These adsorbed dye molecules on the active sites of the semiconductor surface harvest the electrons in the conduction band of photocatalysts, leading to the formation of radical anions from the dyes and the degradation of the dye [46-48]. In other words, this process causes further oxidation, reduces the steps involved in CdO photocatalysation and, finally, degrades organic molecules.

Therefore, the adsorption of either cationic dye or anionic dyes on the surface of the semiconductor plays an important role in the efficiency of their degradation. This is because the percentage of the pollutants decolourized depends on the number and structure of the photocatalyst sites. This study sought to prepare CdO rhombus structures to increase the amount of contact sites and the number of available sites in accordance with the sharp edges of the rhombus structure.

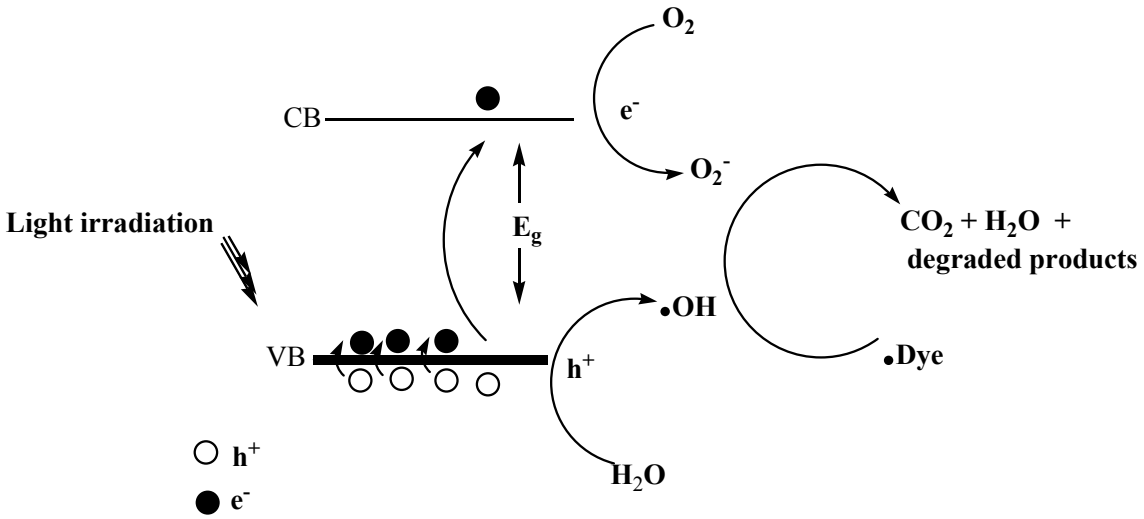

Scheme 3. The diagram of the photocatalytic mechanism of the prepared sample

We found that only MG and CV as cationic dyes and CR as an anionic dye are easily adsorbed on the surface of the CdO nanostructure and broken down into a harmless species. The comparison of the removal efficiency obtained for this product relative to other semiconductors for the photodegradation of these azo dyes revealed that the ability of this metal oxide with the special morphology is similar to the other reported semiconductors [26-34, 45-49].

4. Conclusions

In summary, a rhombus-shaped structure of CdO was successfully synthesized using a facile hydrothermal method and then calcination treatment at 450 ˚C for 2 h. The SEM images clearly revealed the rhombus-like structure of the product including uniform nanoparticles with an average size of 29 nm. We conclude that these nanoparticles are arranged in special orientations and form the rhomboid morphology**.** This study indicated that the CdO as-prepared can be used as a suitable photocatalyst with a qualified efficiency to remove the various azo dyes from aqueous solutions in high concentrations (5–50 $mg.L^{-1}$). This result proved the close relationship between the optical band gap, the structural morphology and photocatalytic properties. The semiconductor prepared was prone to break down the coloured pollutants as a result of a redox process during light illumination. Likewise, the product revealed a good reusability for the photodegradation of the selected dyes after being recycled three times. Accordingly, this type of photocatalyst with its special structure is a promising candidate for further studies.

5. Acknowledgements

The financial support for this study, from the Iran University of Science and Technology and the Iranian Nanotechnology Initiative, is gratefully acknowledged. The authors would like to express their sincere gratitude to Lachin Rezaiian for kindly helping with the editing of the paper.

6. References

[1] El-Sharkawy EA, Soliman AY, Al-Amer KM (2007) Comparative study for the removal of methylene blue via adsorption and photocatalytic degradation. J. Colloid Interface Sci. 310: 498-508.

[2] Zhu HY, Fu YQ, Jiang R, Jiang JH, Xiao L, Zeng GM, Zhao SL, Wang Y (2011) Adsorption removal of Congo Red onto magnetic cellulose/Fe_3O_4/activated carbon composite: Equilibrium, kinetic and thermodynamic studies. Chem. Eng. J. 173: 494-502.

[3] Verma AK, Dash R, Bhunia P (2012) A review on chemical coagulation/ flocculation technologies for removal of colour from textile wastewaters. J. Environ. Manag. 93: 154-168.

[4] Cheng Sh, Oatley DL, Williams PM, Wright CJ (2012) Characterization and application of a novel positively charged nanofiltration membrane for the treatment of textile industry wastewaters. Water. Res. 46: 33-42.

[5] Rahimi R, Kerdari H, Rabbani M, Shafiee M (2011) Synthesis, characterization and adsorbing properties of hollow Zn-Fe_2O_4 nanospheres on removal of Congo Red from aqueous solution. Desalination 280: 412-418.

[6] Afkhami A, Moosavi R (2010) Adsorptive removal of Congo Red, a carcinogenic textile dye, from aqueous solutions by maghemite nanoparticles J. Hazard. Mater. 174: 398-403.

[7] Umar A, Chauhan MS, Chauhan S, Kumar R, Kumar G, Al-Sayari SA, Hwang SW, Al-Hajry A (2011) Large-scale synthesis of ZnO balls made of fluffy thin nanosheets by simple solution process: Structural, optical and photocatalytic properties. J. Colloid Interface Sci. 363: 521-528.

[8] Sun L, Zhao D, Song Z, Shan C, Zhang Z, Li B, Shen D (2011) Gold nanoparticles modified ZnO nanorods with improved photocatalytic activity. J. Colloid Interface Sci. 363: 175-181.

[9] Huo R, Kuang Y, Zhao Z, Zhang F, Xu S (2013) Enhanced photocatalytic performances of hierarchical ZnO/$ZnAl_2O_4$ micro-sphere derived from layered double hydroxide precursor spray-dried microsphere. J. Colloid Interf. Sci. 407: 17-21.

[10] Kalathur AS (2005) Cathodic electrodeposition of cadmium oxide, zinc oxide and mixed cadmium oxide-zinc oxide thin films, The University of Texas Press, Arlington.

[11] Dong W, Zhu C (2003) Optical properties of surface-modified CdO nanoparticles. Opt Mater 22: 227-233.

[12] Vinodkumar R, Lethy KJ, Arunkumar PR, Krishnan RR, Pillai NV, Pillai VPM, Philip R (2010) Effect of cadmium oxide incorporation on the microstructural and optical properties of pulsed laser deposited nanostructured zinc oxide thin films. Mater. Chem. Phys. 121: 406-413.

[13] Grado-Caffaro MA, Grado-Caffaro M (2008) A quantitative discussion on band-gap energy and carrier density of CdO in terms of temperature and oxygen partial pressure. Phys. Lett. A 372: 4858-4860.

[14] Gulino A, Compagnini G, Scalisi AA (2003) Large third-order nonlinear optical properties of cadmium oxide thin films. Chem. Mater. 15: 3332-3336.

[15] Ziabari AA, Ghodsi FE (2011) Optoelectronic studies of sol-gel derived nanostructured CdO-ZnO composite films. J. Alloy Compd. 509: 8748-8755.

[16] Yakuphanoglu F (2010) Nanocluster n-CdO thin film by sol-gel for solar cell applications. Appl. Surf. Sci. 257: 1413-1419.

[17] Ranjbar ZR, Morsali A (2011) Ultrasound assisted syntheses of a nano-structured two-dimensional

mixed-ligand cadmium(II) coordination polymer and direct thermolyses for the preparation of cadmium(II) oxide nanoparticles. Polyhedron 30: 929-934.

[18] Varghese N, Panchakarla LS, Hanapi M, Govindaraj A, Rao CNR (2007) Solvothermal synthesis of nanorods of ZnO, N-doped ZnO and CdO. Mater. Res. Bull. 42: 2117-2124.

[19] Ghoshal T, Kar S, De SK (2009) Morphology controlled solvothermal synthesis of $Cd(OH)_2$ and CdO micro/nanocrystals on Cd foil. Appl. Surf. Sci. 255: 8091-8097.

[20] Ashoka S, Chithaiah P, Chandrappa GT (2010) Studies on the synthesis of $CdCO_3$ nanowires and porous CdO powder. Mater. Lett. 64: 173-176.

[21] Tadjarodi A, Imani M (2011) A novel nanostructure of cadmium oxide synthesized by mechanochemical method. Mater. Res. Bull. 46: 1949-1954.

[22] Tadjarodi A, Imani M (2011) Synthesis and characterization of CdO nanocrystalline structure by mechanochemical method. Mater. Lett. 65: 1025-1027.

[23] Karunakaran C, Dhanalakshmi R (2009) Selectivity in photocatalysis by particulate semiconductors. Cent. Eur. J. Chem. 7: 134-137.

[24] Karunakaran C, Dhanalakshmi R, Gomathisankar P, Manikandan G (2010) Enhanced phenol-photodegradation by particulate semiconductor mixtures: Interparticle electron-jump. J. Hazard. Mater. 176: 799-806.

[25] Nezamzadeh-Ejhieh A, Banan Z (2011) A comparison between the efficiency of CdS nanoparticles/zeolite A and CdO/zeolite A as catalysts in photodecolorization of Crystal Violet. Desalination 279: 146-151.

[26] Rahman MM, Khan BS, Marwani HM, Asiri AM, Alamry KA, Rub MA, Khan A, Khan AAP, Azum N (2014) Facile synthesis of doped ZnOCdO nanoblocks as solid-phase adsorbent and efficient solar photo-catalyst applications. J. Ind. Eng. Chem. 20: 2278–2286.

[27] Saravanan R, Shankar H, Prakash T, Narayanan V, Stephen A (2011) ZnO/CdO composite nanorods for photocatalytic degradation of methylene blue under visible light. Mater. Chem. Phys. 125: 277-280.

[28] Fan Y, Deng M, Chen G, Zhang Q, Luo Y, Li D, Meng Q (2011) Effect of calcination on the photocatalytic performance of CdS under visible light irradiation. Journal of Alloys and Compounds 509: 1477-1481.

[29] Afzal Kamboh M, Solangi IB, Sherazi STH, Memon S (2011) A highly efficient calix[4]arene based resin for the removal of azo dyes. Desalination 268: 83-89.

[30] Rauf MA, Meetani MA, Hisaindee S (2011) An overview on the photocatalytic degradation of azo dyes in the presence of TiO_2 doped with selective transition metals. Desalination 276: 13-27.

[31] Eskizeybek V, Sarı F, Gülce H, Gülce A, Avcı A (2012) Preparation of the new polyaniline/ZnO nanocomposite and its photocatalytic activity for degradation of methylene blue and malachite green dyes under UV and natural sun lights irradiations. Appl. Catal B: Environ. 119-120: 197-206.

[32] Melghit K, Al-Rubaei MS, Al-Amri I (2006) Photodegradation enhancement of Congo Red aqueous solution using a mixture of $SnO_2{\cdot}xH_2O$ gel/ZnO powder. J. Photochem. Photobiol. A: Chem. 181: 137-141.

[33] Chen CC, Lu CS, Chung YC, Jan JL (2007) UV light induced photodegradation of Malachite Green on TiO_2 nanoparticles. J. Hazard. Mater. 141: 520-528.

[34] Wahi RK, Yu WW, Liu Y, Mejia ML, Falkner JC, Nolte W, Colvin VL (2005) Photodegradation of Congo Red catalyzed by nanosized TiO_2. J. Mol. Catal. A: Chem. 242: 48-56.

[35] Tadjarodi A, Imani M, Kerdari H (2013) Experimental design to optimize the synthesis of CdO cauliflower-like nanostructure and high performance in photodegradation of toxic azo dyes. Mater. Res. Bull. 48: 935-942.

[36] Medeiros FFP, Moura MFV, Silva AGP, Souza CP, Gomes KKP, Gomes UU (2006) The thermal decomposition of monohydrated ammonium oxotris (oxalate) niobate. Braz. J. Chem. Eng. 23: 531-538.

[37] Pavia DLGL, Kriz GS, Vyvyan JR (2009) Introduction to Spectroscopy, fourth ed., Brooks/cole Cengage Learning, United State.

[38] Nakamoto K (2009) Infrared Raman Spectra of Inorganic and Coordination Compounds, sixth ed., John Wiley & Sons, Inc., Hoboken, New Jersey.

[39] Singh SC, Swarnkar RK, Gopal R (2009) Cadmium oxide nanostructures in water; synthesis, characterizations and optical properties. AIP Conf. Proc. 1147: 211-215.

[40] Tharayil NJ, Raveendran R, Vaidyan A V, Chithra PG (2008) Optical, electrical and structural studies of nickel-cobalt oxide nanoparticles. Indian J. Eng. Mater. Sci. 15: 489-496.

[41] Saleh TA, Gupta VK (2012) Photo-catalyzed degradation of hazardous dye methyl orange by use of a composite catalyst consisting of multi-walled carbon nanotubes and titanium dioxide. J. Colloid Interface Sci. 371: 101-106.

[42] Chandiramouli R, Jeyaprakash BG (2013) Review of CdO thin films. Solid State Sci. 16: 102-110.

[43] Zaien M, Hmood A, Ahmed NM, Hassan Z (2013) Growth and characterization of different structured CdO using a vapor transport. Mater. Lett. 102-103: 12-14.

[44] Aksoy S, Caglar Y, Ilican S, Caglar M (2009) Effect of heat treatment on physical properties of CdO films deposited by sol-gel method. Int. J. hydrogen energy 34: 5191-5195.

[45] Lanje AS, Ningthoujam RS, Sharma SJ, Pode RB (2011) Luminescence and electrical resistivity properties of cadmium oxide nanoparticles. Indian J. Pure Appl. Phys. 49: 234-238.

[46] Xiang Q, Yu J, Jaroniec M (2012) Graphene-based semiconductor photocatalysts. Chem. Soc. Rev. 41: 82-796.

[47] Zhao X, Wang L, Xu X, Lei X, Xu S, Zhang F (2012) Fabrication and photocatalytic properties of novel ZnO/$ZnAl_2O_4$ nanocomposite with $ZnAl_2O_4$ dispersed inside ZnO network. AIChE J. 58: 573-582.

[48] Sapawe N, Jalil AA, Triwahyono S (2013) One-pot electro-synthesis of ZrO_2-ZnO/HY nanocomposite for photocatalytic decolorization of various dye-contaminants. Chem. Eng. J. 225: 254-265.

[49] Ameen S, Akhtar MS, Nazim M, Shin HS (2013) Rapid photocatalytic degradation of Crystal Violet dye over ZnO flower nanomatrials. Mater. Lett. 96: 228-232.